Master thesis in applied physics and mathematics

Control of skyrmion motion via current and inhomogeneous electric fields in thin-film Dzyaloshinskii-Moriya ferromagnets with Rashba spin-orbit coupling

Author:
Øyvind Johansen

Supervisor:
Prof. Jacob Linder

February 22, 2016

NTNU
Norwegian University of
Science and Technology

Abstract

Sammendrag

Preface

Øyvind Johansen
Trondheim, Norway
2016

Contents

1 Introduction

2 Fundamental theory

2.1 Energy terms in micromagnetics

2.1.1 Exchange energy

Ferromagnetism occurs in materials where the spins tend to align with each other, and thereby being able to generate an observable magnetic field outside of the material. The mechanism behind this is the exchange interaction between the spins. In ferromagnetic materials the system can lower its energy by having parallel neighboring spins. This is described by the Heisenberg Hamiltonian,

$$H = -J \sum_{\langle i,j \rangle} \boldsymbol{S}_i \cdot \boldsymbol{S}_j, \tag{2.1}$$

with J being the exchange integral which is positive for ferromagnetic materials and $\boldsymbol{S}$ a dimensionless spin-vector. The spins can be expressed in terms of the magnetization, which is the average magnetic moment. As the magnetic moment and the spin of an electron are anti-parallel, this relation becomes

$$\boldsymbol{S}_i = -\frac{S}{M_s} \boldsymbol{M}_i, \tag{2.2}$$

with M_s being the saturation magnetization and S the magnitude of the spin. The magnetization is a classical vector, and in micromagnetism it is treated as a slowly varying smooth function. One can therefore perform a Taylor expansion of it. By doing that, one can show [1] that the energy density can be written as

$$\epsilon_{EX} = \frac{\mathrm{d}E_{EX}}{\mathrm{d}V} = -\frac{A}{M_s^2} \boldsymbol{M}(\boldsymbol{r}) \nabla^2 \boldsymbol{M}(\boldsymbol{r}) = \frac{A}{M_s^2} \partial_i \boldsymbol{M}(\boldsymbol{r}) \partial_i \boldsymbol{M}(\boldsymbol{r}), \tag{2.3}$$

with A being the exchange stiffness

$$A = \frac{JS^2}{2a} \tag{2.4}$$

and a being the lattice constant.

2.1.2 Perpendicular magnetic anisotropy

In some magnetic materials we may have something known as magnetic anisotropy. As the name indicates, there is an anisotropy in the material that makes certain magnetization directions more energetically favorable than others. This mostly stems from the spin-orbit coupling. If one considers the restframe of the electron instead of the proton, the proton is orbiting the electron and thereby causing a temporal varying electric field. Ampère's ciruital law then says that the electron observes a magnetic field proportional to the orbital motion of the proton. This magnetic field then interacts with the magnetic moment of the electron, which is proportional to the spin, hence the name spin-orbit coupling. Taking this into consideration as well as the atomic structure in the material, one can see that one could end up with a material where the magnetic field the electrons experience from the spin-orbit coupling would allow one direction to be easier magnetized than others.

In some layered ultrathin film structures, such as Pd/Co [2], it has been discovered that the magnetization has a lower energy when it is perpendicular to the films. This means that the easy axis of the material is perpendicular to the films, and we then have something called perpendicular magnetic anisotropy (PMA). The anisotropic energy is independent of the direction the magnetization has along the easy axis, meaning the energy is the same if the magnetization points into or out of the films. Letting K be the anisotropy constant and θ the angle to the normal of the films, the anisotropic energy density can then be written as

$$\epsilon_{PMA} = K \sin^2 \theta \tag{2.5}$$

to the lowest order in θ. Here we have normalized the energy density in such a way that if the magnetization points along the easy axis the energy density is zero.

2.1.3 Voltage induced magnetic anisotropy

One form of perpendicular magnetic anisotropy occurs at the interface between certain materials. This has been attributed to the exchange interaction between $p-$ and $d-$oribitals at material interfaces, such as the $3d$ orbital in Fe and $2p$ orbital in O at an Fe/MgO interface [3]. As this is a magnetic anisotropy that only occurs at the surface of the material, it will only be of importance in ultra-thin magnetic films where surface effects are of a greater importance. It has also been discovered that one can modify the strength of this surface magnetic anisotropy with an external electric field. The reason for the change of strength in the magnetic anisotropy is the modification of the occupation number in the $3d$ orbitals in Fe, thereby affecting the $p - d$ exchange interaction that is the origin of the magnetic surface anisotropy [4]. It was found that in a thin-film system with an Fe/MgO interface where the Fe layer consisted of only a few monoatomic layers a change of approximately 40% could be achieved in the magnetic surface anisotropy by application of an external electric field. As it is relatively easy to generate a localized electric field, one can therefore create an energy landscape to influence the dynamics of magnetization patterns. An example of this was shown by Uphadhyaya et al. by guiding dipole-dipole interaction skyrmions with voltage gates [5].

2.1.4 Rashba spin-orbit coupling

In materials where the motion of the electrons is confined to a plane, and the inversion symmetry is broken along the axis perpendicular to that plane, there is a splitting of the

spin energy levels. Inversion symmetry can for example be broken at the interface between two materials [6]. The inversion asymmetry causes an electric field perpendicular to the plane of motion, as the gradient of the electrostatic potential becomes non-zero when inversion symmetry is broken ($V(\boldsymbol{r}) \neq V(-\boldsymbol{r})$). When particles move in an electric field, they experience a magnetic field which can be seen by performing a Lorentz transformation into the particles' restframe. This magnetic field is proportional to $\boldsymbol{v} \times \boldsymbol{E}$. Because of the magnetic field the energy levels become spin dependent, as the field couples to the spin. This is described by the Rashba Hamiltonian [7]

$$H_R = \frac{\alpha_R}{\hbar} \boldsymbol{\sigma} \cdot (\boldsymbol{p} \times \hat{\boldsymbol{n}}) = \alpha_R (\boldsymbol{\sigma} \times \boldsymbol{k}) \cdot \hat{\boldsymbol{n}}. \tag{2.6}$$

Here α_R is the Rashba parameter, $\boldsymbol{p} = \hbar \boldsymbol{k}$ the momentum of the electrons, $\hat{\boldsymbol{n}}$ a unit vector perpendicular to the plane of motion and $\boldsymbol{\sigma}$ is a vector of the Pauli matrices.

2.1.5 The Dzyaloshinskii–Moriya interaction

The Dzyaloshinskii–Moriya interaction (DMI) is an antisymmetric exchange coupling between spins, given by the Hamiltonian

$$H_{DM} = \sum_{\langle i,j \rangle} \boldsymbol{D}_{ij} \cdot (\boldsymbol{S}_i \times \boldsymbol{S}_j). \tag{2.7}$$

This interaction only occurs in materials where the inversion symmetry is broken. The magnitude of $\boldsymbol{D}_{ij}$ depends on the material properties, and the direction of $\boldsymbol{D}_{ij}$ depends on the symmetry of the atomic structure in the material. Moriya showed [8] that if there is an n-fold axis (with $n \geq 2$) along the axis between the particles with spins $\boldsymbol{S}_i$ and $\boldsymbol{S}_j$, $\boldsymbol{D}_{ij}$ will be parallel to that axis. Using that in a Taylor expansion of (2.7), it can be shown that the energy density becomes

$$\epsilon_{DM}^{(\text{bulk})} = \frac{D}{M_s^2} \boldsymbol{M} \cdot (\nabla \times \boldsymbol{M}). \tag{2.8}$$

On the other hand, if there is a mirror plane located at the center of the line between the particles with spins $\boldsymbol{S}_i$ and $\boldsymbol{S}_j$ that is perpendicular to the axis intersecting them, the vector $\boldsymbol{D}_{ij}$ lies in the mirror plane. In a more specific case where the interaction between the spins $\boldsymbol{S}_i$ and $\boldsymbol{S}_j$ is mediated by a third magnetic particle (different from the other two) located in the mirror plane, $\boldsymbol{D}_{ij}$ is perpendicular to the triangle spanned by the three particles as illustrated in Figure 2.1. Assuming the magnetic particles with spins $\boldsymbol{S}_i$ and $\boldsymbol{S}_j$ are located in the xy-plane, and that the mediating magnetic particle of a different type lies above them, a Taylor expansion of (2.7) yields the energy density

$$\epsilon_{DM}^{(\text{interface})} = \frac{D}{M_s^2} \left[M_z (\nabla \cdot \boldsymbol{M}) - (\boldsymbol{M} \cdot \nabla) M_z \right]. \tag{2.9}$$

The observant reader may have noticed that both the Rashba spin-orbit coupling and Dzyaloshinskii-Moriya interaction occur in materials with inversion asymmetry. Dzyaloshinskii first introduced DMI based on a phenemenological reasoning [9] to describe what had been observed experimentally, and Moriya later proposed that the microscopic mechanism behind this was spin-orbit coupling [8]. In thin-film system it is then reasonable to

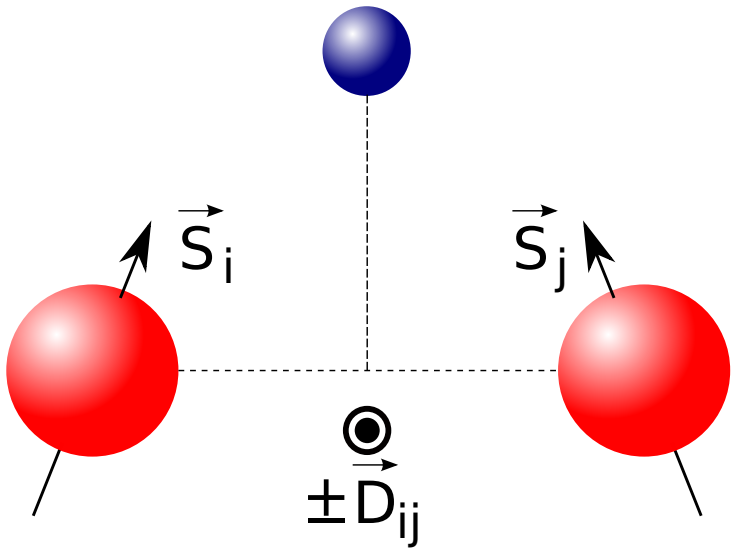

Figure 2.1. An illustration of the geometry of an interfacial DMI. The antisymmetric interaction between the spins $\boldsymbol{S}_i$ and $\boldsymbol{S}_j$ is mediated by a third magnetic particle in blue. The direction of $\boldsymbol{D}_{ij}$ is then perpendicular to the plane spanned by the three particles.

assume that Rashba spin-orbit coupling can be the mechanism behind DMI. This was in fact shown mathematically by Kim *et al.* [10]. They started with the model Hamiltonian

$$H = H_{\text{kin}} + H_R + H_E = \frac{\boldsymbol{p}^2}{2m_e} + \frac{\alpha_R}{\hbar}\boldsymbol{\sigma}\cdot(\boldsymbol{p}\times\hat{\boldsymbol{n}}) + J\boldsymbol{\sigma}\cdot\hat{\boldsymbol{M}} \tag{2.10}$$

that includes the kinetic energy of electrons confined to a plane, a Rashba spin-orbit coupling and the symmetric exchange energy between the spins. A unitary transformation was then performed on the Hamiltonian to remove the explicit Rashba Hamiltonian from the model, so that the transformed Hamiltonian could be written as $H' = U^\dagger H U = H_{\text{kin}} + H'_E + \mathcal{O}(\alpha_R^2)$. This unitary transformation, defined by

$$U = \exp\left[-i\frac{\alpha_R m_e}{\hbar^2}\boldsymbol{\sigma}\cdot(\boldsymbol{r}\times\hat{\boldsymbol{n}})\right], \tag{2.11}$$

does not change the eigenvalues of the system, and the physics in the transformed Hamiltonian is therefore the same as the original model Hamiltonian. It was then shown that the transformed symmetric exchange energy included an interfacial DMI term with the strength of the parameter D being

$$D = \frac{4\alpha_R m_e A}{\hbar^2}. \tag{2.12}$$

2.2 Skyrmions

In certain types of materials, such as chiral magnets, an exotic magnetization pattern has been found to occur. This magnetization pattern, known as a skyrmion, is a vortex-like magnetization structure with non-trivial topology. The magnetization of the skyrmion wraps around the unit sphere, meaning that it has a non-zero skyrmion number [11]

$$N_{\text{sk}} = \frac{1}{4\pi}\int \hat{\boldsymbol{M}}\cdot(\partial_x\hat{\boldsymbol{M}}\times\partial_y\hat{\boldsymbol{M}})\,\mathrm{d}x\,\mathrm{d}y. \tag{2.13}$$

Skyrmions have an integer skyrmion number, while vortices have a half-integer skyrmion number [12]. The magnetization of the skyrmion can be written in cartesian coordinates as

$$\boldsymbol{M}(\rho,\phi) = M_s \begin{pmatrix} \cos\Phi(\phi)\sin\theta(\rho) \\ \sin\Phi(\phi)\sin\theta(\rho) \\ \cos\theta(\rho) \end{pmatrix}. \tag{2.14}$$

As the out-of-plane component (here the z-component) of the magnetization in the skyrmion is rotationally symmetric around the skyrmion's core, the out-of-plane angle θ can be written as a function of ρ only, with ρ being the distance to the skyrmion's core. The in-plane magnetization angle Φ is assumed to be a linear function of the azimuthal angle ϕ, such that

$$\Phi = m\phi + \psi. \tag{2.15}$$

Due to the periodical nature of the angles, m is constrained to be an integer. The phase difference ψ between Φ and ϕ is a constant called the helicity of the skyrmion. If one plugs in the ansatz (2.14) into (2.13), one finds that

$$N_{\text{sk}} = \frac{m}{4\pi}\int_0^{2\pi} \mathrm{d}\phi \int_0^{\infty} \mathrm{d}\rho \sin\theta(\rho)\frac{\partial\theta(\rho)}{\partial\rho} = -\frac{m}{2}\cos(\theta(\rho))|_{(\rho=0)}^{(\rho=\infty)}. \tag{2.16}$$

Unless m is an even number, one must require that $\theta(\rho=0)=0$ and $\theta(\rho=\infty)=\pi$, or $\theta(\rho=0)=\pi$ and $\theta(\rho=\infty)=0$ for the skyrmion number to be an integer and not a half-integer.

The skyrmion needs a certain type of physical mechanism in the material to be a stable state. This mechanism will allow a lower energy state by having the neighbouring spins not be entirely parallel to each other, like the symmetric exchange interaction wants them to be. One of these mechanisms is the Dzyaloshinskii–Moriya interaction, which is the stabilizing mechanism of skyrmions we will consider in this thesis. Other mechanisms that can also cause the magnetic skyrmion to be a stable state are long-ranged magnetic dipolar interactions [13], frustrated exchange interactions [14] and four-spin exchange interactions [11]. If we consider the interfacial DMI energy density in (2.9) and plug in our ansatz for the magnetization of the skyrmion, one finds that

$$\epsilon_{DM}^{(\text{interface})} = D\cos((m-1)\phi+\psi)\left(\frac{\partial\theta}{\partial\rho} + \frac{m}{\rho}\sin\theta\cos\theta\right). \tag{2.17}$$

For the DMI to have a net energy contribution, we must remove the dependence on ϕ as the average of a harmonic function over the plane will be zero. We therefore require that $m=1$, which is not an even number, meaning we must apply the boundary conditions for $\theta(\rho)$ mentioned earlier. The helicity ψ is then chosen to minimize the energy contribution from DMI, which leaves us with the two options $\psi=0$ and $\psi=\pi$, depending on the sign of D and the θ profile. Due to the boundary conditions for θ, the magnetization in the core of the skyrmion points in the opposite direction of the magnetization far away from the skyrmion core. The magnetization direction far away from the core must therefore be a stable direction in the energy. This can be done in a system with an easy axis parallel to that direction. If we consider a skyrmion in a thin film, which makes sense with our choice of interfacial DMI, the easy axis must be perpendicular to that film. In other words, we need a thin-film system with perpendicular magnetic anisotropy. Finally, as our system is

ferromagnetic, we also need to include the symmetric exchange interaction. This is also necessary if we want to treat the skyrmion in the micromagnetic model, where we assume that the magnetization can be estimated by a smooth function. This assumption was for example used in the Taylor expansion of the DMI Hamiltonian. Our model then has the energy density given by

$$\begin{aligned}\epsilon &= \epsilon_E + \epsilon_{PMA} + \epsilon_{DM}^{(\text{interface})} \\ &= A\left[\left(\frac{\partial\theta}{\partial\rho}\right)^2 + \frac{\sin^2\theta}{\rho^2}\right] + K\sin^2\theta + D\cos\psi\left(\frac{\partial\theta}{\partial\rho} + \frac{1}{\rho}\sin\theta\cos\theta\right),\end{aligned} \tag{2.18}$$

assuming a magnetization profile given by (2.14). The energy is independent of ϕ due to our choice of m, but it remains a function of θ and ρ. As the skyrmion is a ground state, we can find the function $\theta(\rho)$ by minimizing the energy. Using the condition

$$\frac{\delta\epsilon(\theta,\rho)}{\delta\theta(\rho)} = \frac{\partial\epsilon}{\partial\theta} - \frac{\mathrm{d}}{\mathrm{d}\rho}\frac{\partial\epsilon}{\partial(\frac{\partial\theta}{\partial\rho})} = 0 \tag{2.19}$$

and introducing the dimensionless length $\tilde{\rho} = \rho D/A$, one ends up with the following differential equation for $\theta(\rho)$:

$$\frac{\partial^2\theta}{\partial\tilde{\rho}^2} + \frac{1}{\tilde{\rho}}\frac{\partial\theta}{\partial\tilde{\rho}} - \frac{\sin\theta\cos\theta}{\tilde{\rho}^2} + \cos\psi\frac{\sin^2\theta}{\tilde{\rho}} - \frac{AK}{D^2}\sin\theta\cos\theta = 0. \tag{2.20}$$

Definining the ratio AK/D^2 as a parameter C, one can solve this equation numerically for a given C. Some numerical solutions are shown in Figure 2.2 when the boundary conditions $\theta(\rho = 0) = \pi$ and $\theta(\rho = \infty)$ have been used. It should be noted that this differential equation only has a solution when $\cos\psi = 1$ for the chosen boundary conditions. The solutions for the different helicities $\psi_1 = 0$ and $\psi_2 = \pi$ have a simple relation, however. This relation can be verified to be

$$\theta_{\psi_1}(\rho) = \pi - \theta_{\psi_2}(\rho), \tag{2.21}$$

as $\cos\psi$ is antisymmetric under a swap in helicities, and $\frac{\partial^2\theta}{\partial\tilde{\rho}^2}$, $\frac{\partial\theta}{\partial\tilde{\rho}}$, $\cos\theta_{\psi_i}$ are all antisymmetric under the relation above. The two different skyrmions for the two different choices in helicities ψ are illustrated in Figure 2.3. This type of skyrmions is called a hedgehog skyrmion, due to the magnetization pattern that curves into or away from the core.

2.3 Magnons

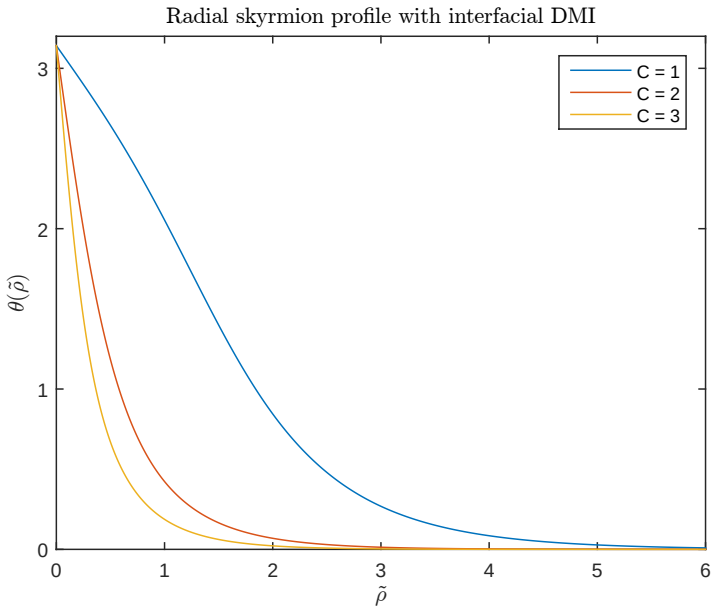

Figure 2.2. The solution of the out-of-plane angle θ of the skyrmion profile for different values of C.

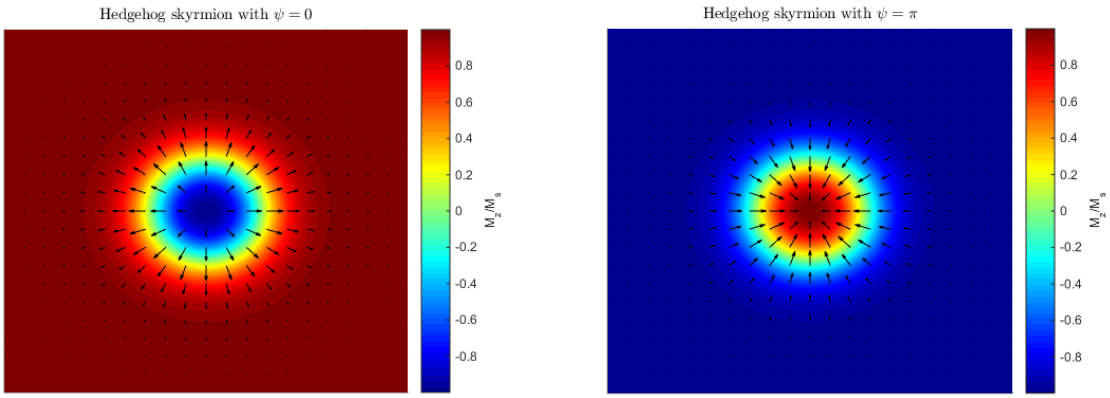

(a) **(b)**

Figure 2.3. A hedgehog skyrmion with a helicity (a) $\psi = 0$ and (b) $\psi = \pi$. The in-plane component of the magnetization is visualized by the vectors, while the z-component is shown in the background color.

3 Magnetization dynamics

3.1 The Landau–Lifshitz–Gilbert equation

Magnetic moments are known to precess around magnetic fields when they are not perfectly aligned. This is known as Larmor precession. The magnetization in a magnet will therefore also perform Larmor precession, as the magnetization is the magnetic moment in a unit volume. This precession can be described by

$$\frac{\mathrm{d}\boldsymbol{M}}{\mathrm{d}t} = -\gamma \boldsymbol{M} \times \boldsymbol{H}, \tag{3.1}$$

where γ is the gyromagnetic ratio defined by

$$\gamma = \frac{g_e \mu_B}{\hbar} \tag{3.2}$$

and $g_e \approx 2$ is the g-factor and μ_B is the Bohr magneton. In addition to performing a precessing motion around the magnetic field, the magnetization will eventually relax parallel to the field to minimize the energy of the system. This can be modeled by introducing a damping term that is perpendicular to the magnetization and the precession of the magnetization. The precessional and damped precessional motions are illustrated in Figure 3.1. Originally Landau and Lifshitz proposed [15] a damping term of the form

$$\frac{\mathrm{d}\boldsymbol{M}}{\mathrm{d}t} = -\gamma \boldsymbol{M} \times (\boldsymbol{H} + \frac{\alpha}{M_s} \boldsymbol{M} \times \boldsymbol{H}), \tag{3.3}$$

but it was discovered that this did not agree well with experiments in systems with a large damping parameter α. Therefore Gilbert proposed a damping term that included the time-derivative of the magnetization instead [16], which agreed much better with experiments, of the form

$$\frac{\mathrm{d}\boldsymbol{M}}{\mathrm{d}t} = -\gamma \boldsymbol{M} \times \boldsymbol{H} + \frac{\alpha}{M_s} \boldsymbol{M} \times \frac{\mathrm{d}\boldsymbol{M}}{\mathrm{d}t}. \tag{3.4}$$

This is known as the Landau–Lifshitz–Gilbert equation. It should be noted that the

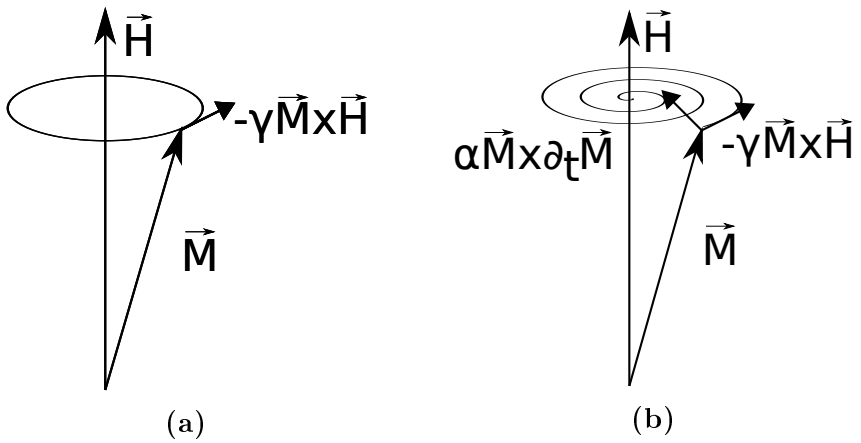

Figure 3.1. The precession of the magnetization vector around a magnetic field. In (a) the precession is undamped and so the magnetization performs counter-clockwise circular rotations around the magnetic field. In (b) the damping component pointing towards the magnetic field causes a spiralling motion of the magnetization vector that eventually aligns the magnetization with the magnetic field.

magnetic field $\boldsymbol{H}$ that the magnetization precesses around is not only an external magnetic field applied to the system, but it's the effective magnetic field experienced locally by the magnetization. The direction of this magnetic field represents the direction in which the magnetization will have a minimum in the micromagnetic energy, and the effective field can therefore be written in terms of the micromagnetic energy. The effective field in the absence of an external field is given by

$$\begin{aligned}\boldsymbol{H}_{\text{eff}} &= -\frac{1}{\mu_0}\frac{\delta\epsilon[\boldsymbol{M}]}{\delta\boldsymbol{M}} \\ &= \frac{2A}{\mu_0 M_s}\nabla^2\boldsymbol{m} + \frac{2(K+\eta E)}{\mu_0 M_s}m_z\hat{\boldsymbol{z}} + \frac{2D}{\mu_0 M_s}\left(\frac{\partial m_z}{\partial x}\hat{\boldsymbol{x}} + \frac{\partial m_z}{\partial y}\hat{\boldsymbol{y}} - (\nabla\cdot\boldsymbol{m})\hat{\boldsymbol{z}}\right),\end{aligned} \tag{3.5}$$

with $\boldsymbol{m}$ being a unit vector in the direction of the magnetization. Here the symmetric exchange interaction, perpendicular and voltage induced magnetic anisotropy and interfacial DMI have been taken into consideration in the effective field.

3.2 Symmetries

3.2.1 Time reversal

3.2.2 Spatial inversion

3.3 The Thiele equation

In the special case of a time-dependent magnetization pattern that can be written as $\boldsymbol{M}(\boldsymbol{r}-\boldsymbol{R}(t))$, Thiele recognized [17] that the time derivative can be written as

$$\frac{\mathrm{d}\boldsymbol{M}}{\mathrm{d}t} = \frac{\partial\boldsymbol{R}}{\partial t}\frac{\partial\boldsymbol{M}}{\partial\boldsymbol{R}} = \frac{\partial\boldsymbol{R}}{\partial t}(-\frac{\partial\boldsymbol{M}}{\partial\boldsymbol{r}}) = -(\boldsymbol{v}\cdot\nabla)\boldsymbol{M}. \tag{3.6}$$

The form $\boldsymbol{M}(\boldsymbol{r}-\boldsymbol{R}(t))$ indicates that the magnetization pattern performs a translation without deformation of the original magnetization profile. Once the equilibrium profile at

some time t_0 is known, the motion of the entire magnetization pattern can be described by the time-dependent position of some distinct part of the magnetization pattern, like the skyrmion-core. If one replaces all time derivatives with Thiele's relation as given above in the LLG equation, one can rewrite the LLG equation to the Thiele equation (as shown by Krüger in [18]):

$$\boldsymbol{F} + \boldsymbol{G} \times (\boldsymbol{v} + b_J \hat{\boldsymbol{j}}_e) + D(\alpha \boldsymbol{v} + \xi b_J \hat{\boldsymbol{j}}_e) = 0. \tag{3.7}$$

This is a force equation with the definitions

$$\boldsymbol{F} = -\frac{\partial E}{\partial \boldsymbol{R}} = -\mu_0 \int \mathrm{d}V \sum_k (\nabla M_k)(H_k), \tag{3.8a}$$

$$\boldsymbol{G} = \frac{2\pi M_s \mu_0 d}{\gamma'} \left[\cos\theta\right]_{\theta(r=0)}^{\theta(r=\infty)} \hat{\boldsymbol{z}}, \tag{3.8b}$$

$$D = -\frac{\pi M_s \mu_0 d}{\gamma'} \int_0^\infty \mathrm{d}r \left(r \left(\frac{\partial \theta}{\partial r} \right)^2 + \frac{\sin^2\theta}{r} \right), \tag{3.8c}$$

where d is the thickness of the film. The vector $\boldsymbol{F}$ is a force originating from an inhomogenous energy landscape or a magnetic field that is not parallel to the local magnetization (in other words a field not aligned with the effective field). $\boldsymbol{G}$ is a gyrovector that only depends on the direction of the magnetization in the skyrmion core and far away from the core. Lastly, D denotes the strength of a dissipative force and is dependent on the radial profile of the out-of-plane angle θ of the skyrmion.

4

Electric control of skyrmion motion

$$\frac{\partial \boldsymbol{M}}{\partial t} = -\gamma' \boldsymbol{M} \times (\boldsymbol{H}_{\text{eff}} + \boldsymbol{H}_R - \frac{\beta}{M_s} \boldsymbol{M} \times \boldsymbol{H}_R) + \frac{\alpha}{M_s} \boldsymbol{M} \times \frac{\partial \boldsymbol{M}}{\partial t} + b_J (\hat{\boldsymbol{j}}_e \cdot \nabla) \boldsymbol{M} - \beta b_J \boldsymbol{M} \times (\hat{\boldsymbol{j}}_e \cdot \nabla) \boldsymbol{M}, \tag{4.1}$$

$$\boldsymbol{H}_R = \frac{\alpha_R m_e}{\hbar \mu_B} b_J (\hat{\boldsymbol{z}} \times \hat{\boldsymbol{j}}_e) = C_R b_J (\hat{\boldsymbol{z}} \times \hat{\boldsymbol{j}}_e). \tag{4.2}$$

$$\boldsymbol{F}_R = -\mu_0 \int \mathrm{d}V \sum_k (\nabla M_k) \left[\boldsymbol{H}_R - \frac{\beta}{M_s} \boldsymbol{M} \times \boldsymbol{H}_R \right]_k \tag{4.3}$$

$$= -\mu_0 \pi \beta C_R b_J M_s d \int_0^\infty \mathrm{d}r \left(\frac{\partial \theta}{\partial r} r + \sin\theta \cos\theta \right) \hat{\boldsymbol{x}} \tag{4.4}$$

$$- \mu_0 \pi C_R b_J M_s d \int_0^\infty \mathrm{d}r \left(r \frac{\partial \theta}{\partial r} \cos\theta + \sin\theta \right) \hat{\boldsymbol{y}} \tag{4.5}$$

$$= -\mu_0 \pi \beta C_R b_J M_s d \int_0^\infty \mathrm{d}r \left(\frac{\partial \theta}{\partial r} r + \sin\theta \cos\theta \right) \hat{\boldsymbol{x}}. \tag{4.6}$$

$$\int_0^\infty \mathrm{d}r \sin\theta(r) = r \sin\theta(r)|_{r=0}^{r=\infty} - \int_0^\infty \mathrm{d}r r \frac{\partial \theta}{\partial r} \cos\theta(r) \tag{4.7}$$

$$\int_0^\infty \mathrm{d}r \left(r \frac{\partial \theta}{\partial r} \cos\theta + \sin\theta \right) = r \sin\theta(r)|_{r=0}^{r=\infty} = 0. \tag{4.8}$$

$$\epsilon_{EF} = \eta E(\boldsymbol{r}) \left(1 - m_z^2\right) = \eta E(\boldsymbol{r}) \sin^2\theta. \tag{4.9}$$

$$E(\boldsymbol{r}) = E_x x + E_y y \tag{4.10}$$

$$= E_x x_0 + E_y y_0 + E_x r \cos\phi + E_y r \sin\phi. \tag{4.11}$$

$$U_{EF} = \int \mathrm{d}V \epsilon_{EF} \tag{4.12}$$

$$= \eta \int_0^d \mathrm{d}z \int_0^{2\pi} \mathrm{d}\phi \int_0^\infty \mathrm{d}r \left(E_x x_0 + E_y y_0 + E_x r\cos\phi + E_y r \sin\phi\right) r \sin^2\theta \tag{4.13}$$

$$= 2\pi\eta d \left(E_x x_0 + E_y y_0\right) \int_0^\infty \mathrm{d}r r \sin^2\theta. \tag{4.14}$$

$$\boldsymbol{F}_E = -\nabla U_{EF} \tag{4.15}$$

$$= -2\pi\eta d \left(E_x \hat{\boldsymbol{x}} + E_y \hat{\boldsymbol{y}}\right) \int_0^\infty \mathrm{d}r r \sin^2\theta. \tag{4.16}$$

$$\boldsymbol{F}_R + \boldsymbol{F}_E + \boldsymbol{G} \times \left(\boldsymbol{v} + b_J \hat{\boldsymbol{j}}_e\right) + D\left(\alpha \boldsymbol{v} + \beta b_J \hat{\boldsymbol{j}}_e\right) = 0. \tag{4.17}$$

$$\boldsymbol{G} = \frac{2\pi M_s \mu_0 d}{\gamma'} \left[\cos\theta\right]_{\theta(r=0)}^{\theta(r=\infty)} \hat{\boldsymbol{z}} \tag{4.18}$$

$$D = -\frac{\pi M_s \mu_0 d}{\gamma'} \int_0^\infty \mathrm{d}r \left(r \left(\frac{\partial\theta}{\partial r}\right)^2 + \frac{\sin^2\theta}{r}\right). \tag{4.19}$$

$$\alpha_C = \frac{\alpha}{4} \int_0^\infty \mathrm{d}r \left(r \left(\frac{\partial\theta}{\partial r}\right)^2 + \frac{\sin^2\theta}{r}\right), \tag{4.20}$$

$$\beta_C = \frac{\beta}{4} \int_0^\infty \mathrm{d}r \left(r \left(\frac{\partial\theta}{\partial r}\right)^2 + \frac{\sin^2\theta}{r}\right), \tag{4.21}$$

$$R = \frac{\gamma' \beta C_R}{4} \int_0^\infty \mathrm{d}r \left(\frac{\partial\theta}{\partial r} r + \sin\theta\cos\theta\right), \tag{4.22}$$

$$C_E = \frac{\gamma'\eta}{2\mu_0 M_s} \int_0^\infty \mathrm{d}r r \sin^2\theta. \tag{4.23}$$

$$\dot{x}_0 = -\frac{1 + \alpha_C\beta_C + R}{1 + \alpha_C^2} b_J + \frac{C_E}{1+\alpha_C^2} E_y - \frac{\alpha_C C_E}{1+\alpha_C^2} E_x, \tag{4.24}$$

$$\dot{y}_0 = \frac{\alpha_C - \beta_C - R}{1 + \alpha_C^2} b_J - \frac{C_E}{1+\alpha_C^2} E_x - \frac{\alpha_C C_E}{1+\alpha_C^2} E_y. \tag{4.25}$$

4.1 Pinning

As with domain walls, there is also a threshold current or field that is necessary for skyrmions to start moving, even though our previous results do not reflect this. In the case of skyrmions this threshold current is much weaker than the case of domain walls [19]. The reason for this reluctance to move is pinning centers, which have much less impact on the motion of skyrmions than that of domain walls, but have an impact nonetheless. To model the effect of pinning centers on skyrmion motions at low current densities or

weak electric fields, one can introduce a pinning force in the Thiele equation (3.7). The equation of interest then becomes

$$\boldsymbol{F}_{\text{pin}} + \boldsymbol{F}_R + \boldsymbol{F}_E + \boldsymbol{G} \times \left(\boldsymbol{v} + b_J \hat{\boldsymbol{j}}_e\right) + D\left(\alpha \boldsymbol{v} + \beta b_J \hat{\boldsymbol{j}}_e\right) = 0. \tag{4.26}$$

The pinning force $\boldsymbol{F}_{\text{pin}}$ is usually written as [20, 21].

$$\boldsymbol{F}_{\text{pin}} = -4\pi v_{\text{pin}} f(\frac{v}{v_{\text{pin}}}) \frac{\boldsymbol{v}}{v}, \tag{4.27}$$

where the function $f(\frac{v}{v_{\text{pin}}})$ goes towards unity for small skyrmion velocities v. In the low velocity limit one therefore approximates the pinning force by

$$\boldsymbol{F}_{\text{pin}} = -v_{\text{pin}} \frac{\boldsymbol{v}}{v}, \tag{4.28}$$

where the forces are normalized in a way so that the gyrovector $\boldsymbol{G} = (0, 0, 1)$. If one plugs this into the Thiele equation given by (4.26) and solves for the total velocity v, one ends up with the result

$$\begin{aligned} v = &\big(\big[\alpha_C^2 v_{\text{pin}}^2 - (\alpha_C^2 + 1)(v_{\text{pin}}^2 - \beta_C^2 b_J^2 + 2\beta_C (C_E E_x + R b_J) b_J - (C_E E_x + R b_J)^2 \\ &- b_J^2 - 2 C_E E_y b_J - C_E^2 E_y^2)\big]^{\frac{1}{2}} - \alpha_C v_{\text{pin}}\big) / \big(\alpha_C^2 + 1\big). \end{aligned} \tag{4.29}$$

From this expression one can then determine the threshold current or electric field gradient necessary for the solution of v to be greater than zero. If we first consider the case where the skyrmion motion is solely driven by a spin-polarized current, one finds that the skyrmion moves when $b_J > b_J^{(\text{crit})}$ with

$$b_J^{(\text{crit})} = \frac{1}{1 + \beta^2} \frac{\mu_B P}{e M_s} j_e^{(\text{crit})} = \frac{v_{\text{pin}}}{\sqrt{\beta_C^2 - 2\beta_C R + R^2 + 1}}. \tag{4.30}$$

In the field driven case where the skyrmion motion is solely driven by an inhomogenous electric field applied perpendicular to the film, one finds that the skyrmion moves when the field gradient $E_g = \sqrt{E_x^2 + E_y^2}$ is greater than some critical value

$$E_g^{(\text{crit})} = \frac{v_{\text{pin}}}{C_E}. \tag{4.31}$$

Up unto this point we have only discussed the total velocity as a result of pinning, and not the individual velocity components $\dot{x}_0$ and $\dot{y}_0$. These are rather simple to find once the total velocity v is known. If one compares the form of $\boldsymbol{F}_{\text{pin}}$ to the form of the dissipative force in (4.26), one sees that the pinning force can be included in the dissipative force. To get the velocity components in the presence of a pinning site one therefore makes the substitution

$$\alpha_C \to \alpha_C + \frac{v_{\text{pin}}}{v} \tag{4.32}$$

into the expressions for $\dot{x}_0$ and $\dot{y}_0$. As one can see from this expression, the pinning is the most influential when the skyrmion is barely moving. As the skyrmion reaches a velocity much greater than the pinning velocity v_{pin}, the effects of the pinning center becomes negligible.

5

Magnon induced skyrmion motion

6
Conclusion

7 Bibliography

[1] Ø. Johansen. Magnetization dynamics of domain walls and skyrmions in micromagnetics. `https://github.com/oyvindjohansen/Ferromagnetism-DW/blob/master/main.pdf`.

[2] P. F. Carcia, A. D. Meinhaldt, and A. Suna. Perpendicular magnetic anisotropy in Pd/Co thin film layered structures. *Applied Physics Letters*, 47(2), 1985.

[3] Fumihiro Matsukura, Yoshinori Tokura, and Hideo Ohno. Control of magnetism by electric fields. *Nat Nano*, 10(3):209–220, Mar 2015. Review.

[4] T. Maruyama, Y. Shiota, T. Nozaki, K. Ohta, N. Toda, M. Mizuguchi, A. Tulapurkar, T. Shinjo, M. Shiraishi, S. Mizukami, Y. Ando, and Y. Suzuki. Large voltage-induced magnetic anisotropy change in a few atomic layers of iron. *Nat Nano*, 4(3):158–161, Mar 2009.

[5] P. Upadhyaya, G. Yu, P. K. Amiri, and K. L. Wang. Electric-field guiding of magnetic skyrmions. *Phys. Rev. B*, 92:134411, Oct 2015.

[6] M. Heide, G. Bihlmayer, Ph. Mavropoulos, A. Bringer, and S. Blügel. Spin–orbit driven physics at surfaces. *Newsletter of the Psi-K Network*, 78, 2006.

[7] Y. A. Bychkov and E. I. Rashba. Oscillatory effects and the magnetic susceptibility of carriers in inversion layers. *Journal of Physics C: Solid State Physics*, 17(33):6039, 1984.

[8] T. Moriya. Anisotropic superexchange interaction and weak ferromagnetism. *Phys. Rev.*, 120:91–98, Oct 1960.

[9] I. E. Dzyaloshinskii. A Thermodynamic Theory of "Weak" Ferromagnetism of Antiferromagnets. *J. Phys. Chem. Solids*, 4:241–255, 1958.

[10] K-W. Kim, H-W. Lee, K-J. Lee, and M. D. Stiles. Chirality from interfacial spin-orbit coupling effects in magnetic bilayers. *Phys. Rev. Lett.*, 111:216601, Nov 2013.

[11] S. Heinze, K. von Bergmann, M. Menzel, J. Brede, A. Kubetzka, R. Wiesendanger, G. Bihlmayer, and S. Blugel. Spontaneous atomic-scale magnetic skyrmion lattice in two dimensions. *Nat Phys*, 7(9):713–718, September 2011.

[12] O. A. Tretiakov and O. Tchernyshyov. Vortices in thin ferromagnetic films and the skyrmion number. *Phys. Rev. B*, 75:012408, Jan 2007.

[13] Y. S. Lin, P. J. Grundy, and E. A. Giess. Bubble domains in magnetostatically coupled garnet films. *Applied Physics Letters*, 23(8), 1973.

[14] T. Okubo, S. Chung, and H. Kawamura. Multiple-q states and the skyrmion lattice of the triangular-lattice heisenberg antiferromagnet under magnetic fields. *Phys. Rev. Lett.*, 108:017206, Jan 2012.

[15] L. D. Landau and E. M. Lifshitz. On the theory of the dispersion of magnetic permeability in ferromagnetic bodies. *Phys. Zeitsch. der Sow.*, 6:153–169, 1935.

[16] T. L. Gilbert. Classics in Magnetics A Phenomenological Theory of Damping in Ferromagnetic Materials. *IEEE Transactions on Magnetics*, 40(6):3443–3449, November 2004.

[17] A. A. Thiele. Steady-state motion of magnetic domains. *Phys. Rev. Lett.*, 30:230–233, Feb 1973.

[18] B. Krüger. *Current-Driven Magnetization Dynamics: Analytical Modeling and Numerical Simulation*. PhD thesis, Institut für Theoretische Physik Universität Hamburg, 2011.

[19] F. Jonietz, S. Mühlbauer, C. Pfleiderer, A. Neubauer, W. Münzer, A. Bauer, T. Adams, R. Georgii, P. Böni, R. A. Duine, K. Everschor, M. Garst, and A. Rosch. Spin transfer torques in mnsi at ultralow current densities. *Science*, 330(6011):1648–1651, 2010.

[20] Karin Everschor, Markus Garst, Benedikt Binz, Florian Jonietz, Sebastian Mühlbauer, Christian Pfleiderer, and Achim Rosch. Rotating skyrmion lattices by spin torques and field or temperature gradients. *Phys. Rev. B*, 86:054432, Aug 2012.

[21] Junichi Iwasaki, Masahito Mochizuki, and Naoto Nagaosa. Universal current-velocity relation of skyrmion motion in chiral magnets. *Nat Commun*, 4:1463, Feb 2013.